4206 *J. Chem. Eng. Data* **2010,** *55,* 4206–4210

Phase Equilibria, Crystallization, and Microstructural Studies of Naphthalen-2-ol + 1,3-Dinitrobenzene[†]

Tanvi Agrawal,[‡] Preeti Gupta,[§] Shiva Saran Das,*[,§] Ashutosh Gupta,[‡] and Nakshatra Bahadur Singh[||]

Department of Chemistry, U.P. Autonomous College, Varanasi, India, Department of Chemistry, DDU Gorakhpur University, Gorakhpur, India, and Research and Technology Development Centre, School of Engineering and Technology, Sharda University, Greater Noida, India

Phase diagrams of naphthalen-2-ol + 1,3-dinitrobenzene have been investigated by the thaw melt method. The results show the formation of a simple eutectic mixture. Enthalpy of fusion values of pure components and the eutectic mixture were obtained from DSC studies. Linear velocity of solidification of pure components and the eutectic mixture was determined at different undercooling rates. The values of the linear velocity of crystallization indicate the nonideal nature of the eutectic mixture in the melt. The anisotropic and isotropic crystallizations of naphthalen-2-ol, 1,3-dinitrobenzene, and the eutectic mixture were studied. The flexural strengths of the pure components, hypo- and hypereutectics, and eutectic mixture were determined.

Introduction

In modern technology, low cost and better quality materials are in great demand. During recent years, binary organic eutectic systems have widely been used as a model system for predicting various properties of metallic alloys, and considerable interest has developed in the study of solidification behavior of binary organic eutectics.[1−6]

It has been observed that composite materials exhibit the requisite properties which depend on their microstructures.[7] Anisotropic growth is one of the most efficient techniques in the domain of solidification phenomena. Eutectic solidification appears to be simple; however, the mechanism is quite complex, and despite extensive studies on solidification behavior of organic eutectic systems,[8−14] the mechanism has yet not been fully understood. Solidification kinetics, microstructures, and the nature of interactions which are important parameters for controlling the physical and chemical properties of the eutectic alloys[1,15] are not fully understood. In the present paper, attempts have been made to understand the solidification behavior of the naphthalen-2-ol + 1,3-dinitrobenzene eutectic mixture.

Experimental Section

Materials and Their Purification. Naphthalen-2-ol (SD fine chemicals) with mass fraction purity > 0.98 was further purified by distillation under reduced pressure, and 1,3-dinitrobenzene (SIGMA) with mass fraction purity > 0.99 was used without further purification. The purities of compounds were checked by determining their melting points and found to be (394.2 ± 0.1) K and (364.8 ± 0.1) K, respectively. The melting points were comparable to the literature values.[16]

Phase Diagram Studies. The phase diagram of the system was studied by the thaw melt method.[17] In this method, different amounts of naphthalen-2-ol and 1,3-dinitrobenzene were accurately weighed in glass test tubes to prepare mixtures of different compositions. The glass tubes were sealed and then heated to a temperature slightly above the melting temperatures of the components, shaken well, and chilled in ice-cold water. The process of heating and cooling was repeated several times to ensure homogeneous mixing, and finally the tubes were broken. The solid mixtures thus obtained were crushed in glass mortars and ground to fine powders. The thaw and true melting temperatures of mixtures of different mole fractions were recorded with the help of a precision thermometer which could read up to ± 0.1 K. The thaw points and melting points of different mixtures with mean deviations are given in Table 1. These melting points were plotted against composition to construct the phase diagram.

Table 1. Thaw Melting Temperature, Melting Temperature, and Undercooling Temperature Values for the Naphthalen-2-ol + 1,3-Dinitrobenzene Eutectic System[a]

(x_2)	T_{thaw}/K	T_{fus}/K	T_{U}/K
0.0000	-	394.2 ± 0.1	388.0 ± 0.1
0.1014	335.8 ± 0.1	389.2 ± 0.1	380.2 ± 0.1
0.1791	335.8 ± 0.1	385.1 ± 0.1	375.4 ± 0.1
0.3636	335.8 ± 0.1	378.0 ± 0.1	368.2 ± 0.1
0.2985	335.8 ± 0.1	374.2 ± 0.1	362.6 ± 0.1
0.4000	336.0 ± 0.1	365.1 ± 0.1	354.4 ± 0.1
0.4769	335.8 ± 0.1	358.0 ± 0.1	346.8 ± 0.1
0.5000	335.8 ± 0.1	335.0 ± 0.1	344.6 ± 0.1
0.6000	335.8 ± 0.1	343.1 ± 0.1	334.6 ± 0.1
0.6500	-	336.0 ± 0.1	327.6 ± 0.1
0.7742	336.0 ± 0.1	351.7 ± 0.1	343.0 ± 0.1
0.8854	336.0 ± 0.1	360.8 ± 0.1	348.0 ± 0.1
1.0000	-	364.8 ± 0.1	349.6 ± 0.1

[a] T_{thaw} = thaw melting temperature; T_{fus} = melting temperature; and T_{U} = undercooling temperature.

Undercooling Measurements. The undercooling measurements of pure components and their mixtures were determined by the method described earlier.[17] Approximately equal amounts of the pure components and their mixtures of different compositions were taken in different glass tubes, sealed, and then immersed in a liquid paraffin bath maintained at a temperature slightly above their melting temperatures. After complete melting, the heating was stopped, and the bath was allowed to cool at a constant rate (3 K·min^{-1}). The formation of the first

---

[†] Part of the “Sir John S. Rowlinson Festschrift”.

* Corresponding author. E-mail: ssdas2002@rediffmail.com.

[‡] U.P. Autonomous College.

[§] DDU Gorakhpur University.

[||] Sharda University.

10.1021/je100358e © 2010 American Chemical Society

crystallite was observed by a magnifying glass, and each experiment was repeated at least five times. The temperature at which the first crystallite appeared was noted. The difference between the true melting temperature and the temperature at which the first crystallite appeared gave the undercooling values. The undercooling temperatures obtained for the pure components and different mixtures were recorded and are given in Table 1.

Determination of Linear Velocity of Solidification. The linear velocities of crystallization of naphthalen-2-ol, 1,3-dinitrobenzene, and their eutectic mixture at different undercooling temperatures were determined by the method described by Rastogi and Bassi.[18] The measurements were made in U-shaped pyrex glass tubes (length 30 cm and internal diameter 0.6 cm). The pure components and the eutectic mixture in the form of fine powders were filled separately in glass tubes and placed in an oil thermostat maintained at a temperature slightly above their melting temperatures. After complete melting, the oil bath was allowed to cool a few degrees below the melting temperatures of the samples. In each set of experiment performed, a seed crystal of the pure component or the eutectic mixture was separately added in the melt from one end of the U-tube to start the nucleation process. The nucleation and crystallization started linearly in the tube. The time for a definite length of crystallization in the horizontal portion of the tube was then noted.

Microscopic and Microphotographic Studies. Separate glass slides of naphthalen-2-ol, 1,3-dinitrobenzene, the eutectic mixture, and the hypo- and hypereutectic mixtures were prepared by placing small amounts of fine powders on glass slides which were then placed in an oven maintained at a temperature slightly above their melting temperatures to ensure complete melting. Both anisotropic and isotropic growth patterns of the samples were photographed. In anisotropic crystallization, the melts were crystallized by moving separate glass coverslips over them in one direction. However, for isotropic crystallization, small amounts of fine powders of the samples were kept on the glass slides and melted in an oven. The slides were then immediately placed over ice cubes, and glass coverslips were moved over them in one direction to initiate the crystallization. The microphotographs of the crystallized front were recorded with the help of a digital camera attached to an optical microscope (Olympus CHi20) at a suitable magnification.

Flexural Strength Measurements. The flexural strengths of the samples were measured by the method described earlier.[13] The samples were melted in uniform cylindrical glass tubes and then dipped vertically into an ice bath maintained at 273 K, where solidification occurred. The solidified materials in the form of cylinders were then placed on the stand. A small container of known mass was allowed to hang in the middle of the cylindrical sample, where known weights were added to the container slowly until the cylindrical sample got ruptured. Moduli of rupture σ_{fs} of the materials were calculated with the help of eq 1.[19]

$$\sigma_{fs} = \frac{F_f L}{\pi R^3} \tag{1}$$

where F_f is the load at fracture; L is the distance between support points; and R is the specimen radius. The flexural strength values of pure components, the eutectic mixture, and hypo- and hypereutectic mixtures are given in Table 2.

Determination of Enthalpies of Fusion by DSC Studies. Values of enthalpy of fusion of naphthalen-2-ol, 1,3-dinitrobenzene, and the eutectic mixture were determined from the DSC thermograms obtained with the help of a differential scanning calorimeter (METTLER STAR SW 900) in a nitrogen atmosphere at a heating rate of 5 K·min^{-1}.

Table 2. σ_{fs} Values of the Naphthalen-2-ol + 1,3-Dinitrobenzene System

systems	σ_{fs} (MPa)
naphthalen-2-ol	1.86 ± 0.01
1,3-dinitrobenzene	1.32 ± 0.05
naphthalen-2-ol + 1,3-dinitrobenzene eutectic	3.39 ± 0.04
naphthalen-2-ol + 1,3-dinitrobenzene hypoeutectic	1.67 ± 0.01
naphthalen-2-ol + 1,3-dinitrobenzene hypereutectic	2.059 ± 0.01

Results and Discussion

The phase diagram of the naphthalen-2-ol + 1,3-dinitrobenzene system is shown in Figure 1. The phase diagram curve suggests the formation of a eutectic mixture at 0.6500 mol fraction of 1,3-dinitrobenzene (x_2) which melts at (336.0 ± 0.1) K. The spontaneous crystallization data have also been graphically shown in Figure 1, which is similar to the phase diagram curve. In general, crystallization from the melt is a diffusion-controlled process and depends on temperature, crystal habits of components, and their concentrations in the melt phase. One of the basic characteristics of the melt is its tendency to be supercooled. The question is why the macroscopic solidification does not start immediately, when the molten system is cooled to the temperature very slightly below the equilibrium liquidus temperature. This may be due to short-range order in the liquid phase. As soon as the short-range order starts disappearing, nucleation and crystal growth start, and solidification begins.

According to Hillig−Turnbull,[20] the linear velocity of crystallization (v) and undercooling (ΔT) are related by eq 2.

$$v = k(\Delta T)^n \tag{2}$$

where k is the kinetic coefficient, and n is a constant. Straight lines are obtained when log v is plotted against log(ΔT) (Figure 2). From the intercepts and slopes of the straight lines in Figure 2, the values of k and n in each case were calculated. The experimental values of the crystallization parameters, k and n, are given in Table 3, which depend on the solidification behavior

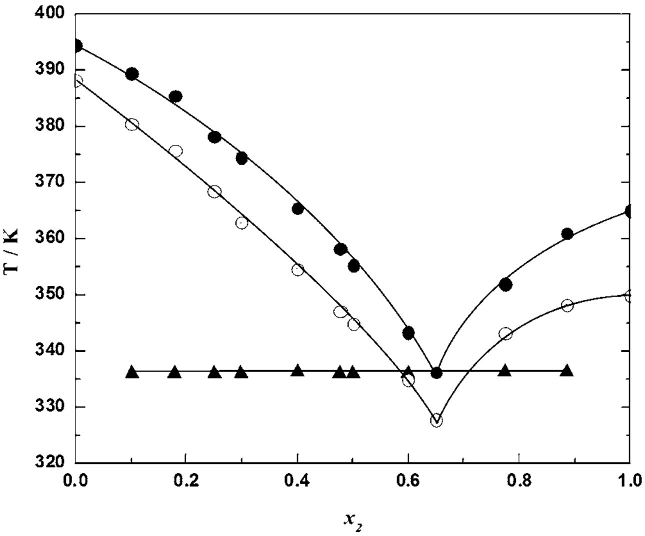

Figure 1. Phase diagram of the naphthalen-2-ol + 1,3-dinitrobenzene eutectic system. ●, Melting temperature; ▲, thaw melting temperature; ○, undercooling temperature.

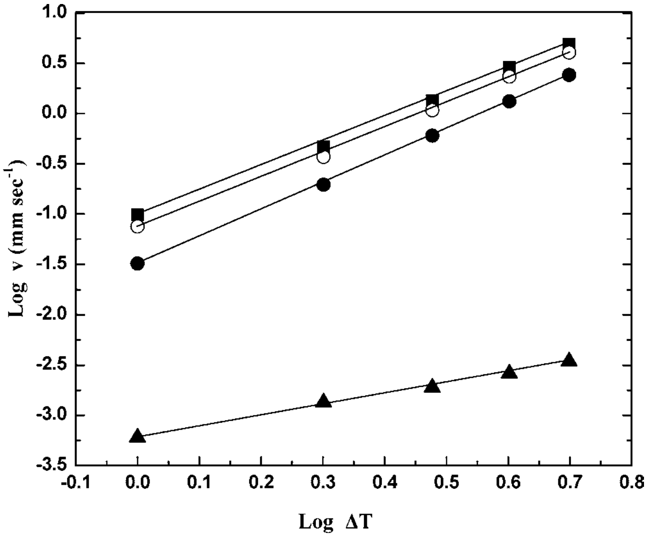

Figure 2. Verification of the $v = k(\Delta T)^n$ equation for the naphthalen-2-ol + 1,3-dinitrobenzene eutectic system. ●, naphthalen-2-ol; ■, 1,3-dinitrobenzene; ▲, eutectic (experimental); ○, eutectic (mixture law).

Table 3. Values of *k* and *n* for the Naphthalen-2-ol + 1,3-Dinitrobenzene Eutectic System

systems	k (mm·s^{-1}·K^{-1})	n
naphthalen-2-ol	0.0322 ± 0.0002	2.685 ± 0.005
1,3-dinitrobenzene	0.0979 ± 0.0022	2.41 ± 0.16
eutectic mixture (experimental)	0.0006 ± 0.0000	1.08 ± 0.00
eutectic mixture (mixture law)	0.0749 ± 0.0015	2.465 ± 0.125

of materials. It is known that the experimental values of n close to 2 indicate the square relationship between the growth velocity and the undercooling. However, in the present system, the values of n are not equal to 2; the values are higher than 2 (for naphthalen-2-ol and 1,3-dinitrobenzene) and lower than 2 (for the eutectic mixture). A value of n less than 2 suggests less rapid variation in the growth velocity with undercooling, while a value greater than 2 suggests more rapid variation in the growth velocity with undercooling, in comparison to the cases where n is equal to 2.

The linear velocity of crystallization (v) for the eutectic mixture was also calculated by using the mixture law (eq 3).

$$v_e = x_1 v_1 + x_2 v_2 \tag{3}$$

where x_1 and x_2 are the mole fractions of components 1 (naphthalen-2-ol) and 2 (1,3-dinitrobenzene), and v_e, v_1, and v_2 are the linear velocities of crystallization of the eutectic mixture, component 1, and component 2, respectively. For the eutectic mixture, a straight line is also obtained when log v (as calculated from the mixture law) is plotted against log ΔT (Figure 2). From Figure 2, it is noticed that the linear velocities of crystallization for the eutectic mixture at different undercoolings, calculated by the mixture law, are higher than the experimental values. It seems that in the eutectic mixture there may exist some sort of weak interaction or molecular association between naphthalen-2-ol and 1,3-dinitrobenzene. Therefore, the eutectic system cannot be considered as a mechanical mixture of the pure components.[21] From Figure 2 it is clear that as the undercooling temperature increases the linear velocity of crystallization also increases, and the experimental values of linear velocities of crystallization of the eutectic mixture are found to be lower than the linear velocities of crystallization of individual components.

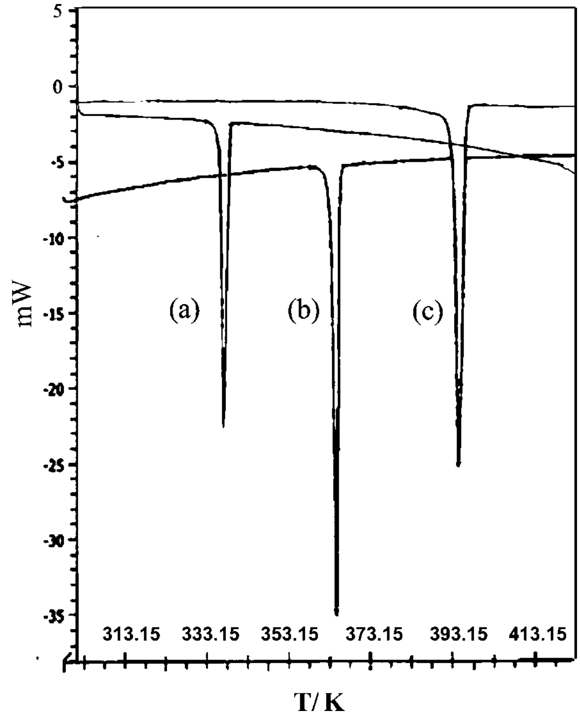

Figure 3. DSC curves for the naphthalen-2-ol + 1,3-dinitrobenzene eutectic system. (a) Naphthalen-2-ol + 1,3-dinitrobenzene eutectic. (b) 1,3-Dinitrobenzene. (c) Naphthalen-2-ol.

Table 4. $\Delta_{fus}H$ and α for the Naphthalen-2-ol + 1,3-Dinitrobenzene Eutectic System

	$\Delta_{fus}H$ (experimental)	$\Delta_{fus}H$ (calculated)	(α)	
systems	kJ·mol^{-1}	kJ·mol^{-1}	$\xi = 0.5$	$\xi = 1.0$
naphthalen-2-ol	21.075	-	3.22	6.43
1,3-dinitrobenzene	21.203	-	3.49	6.99
naphthalen-2-ol + 1,3-dinitrobenzene eutectic	14.726	21.158	3.95	5.27

An attempt has been made to explain this observation on the basis of the mechanism as proposed by Winegard et al.[22] They have suggested that the eutectic solidification starts with the formation of a nucleus of a phase which has a high melting temperature. Its growth continues until the surrounding liquid becomes rich in composition of the other phase. As a result of increase in the concentration, the second phase then also starts nucleating. It has been reported that when the rate of solidification of the eutectic is lower than that of the parent components there is a possibility of alternate nucleation of the two components; therefore, in the present investigation, one can say that in the case of the eutectic the solidification mechanism follows an alternate nucleation of the two components.

The nonideal nature of the eutectic melt, mode of crystallization, and the nature of interaction between the two components could be predicted from the enthalpies of fusion data. The DSC curves of naphthalen-2-ol, 1,3-dinitrobenzene, and the eutectic mixture are shown in Figure 3. The enthalpies of fusion values of the components and the eutectic mixture as determined experimentally from DSC technique and calculated by using a mixture law (eq 4) are given in Table 4.

$$(\Delta_{fus}H)_e = (x_1)_e(\Delta_{fus}H)_1 + (x_2)_e(\Delta_{fus}H)_2 \tag{4}$$

where $(\Delta_{fus}H)_1$ and $(\Delta_{fus}H)_2$ are the enthalpies of fusion of components 1 and 2, respectively. Equation 4 is just to know

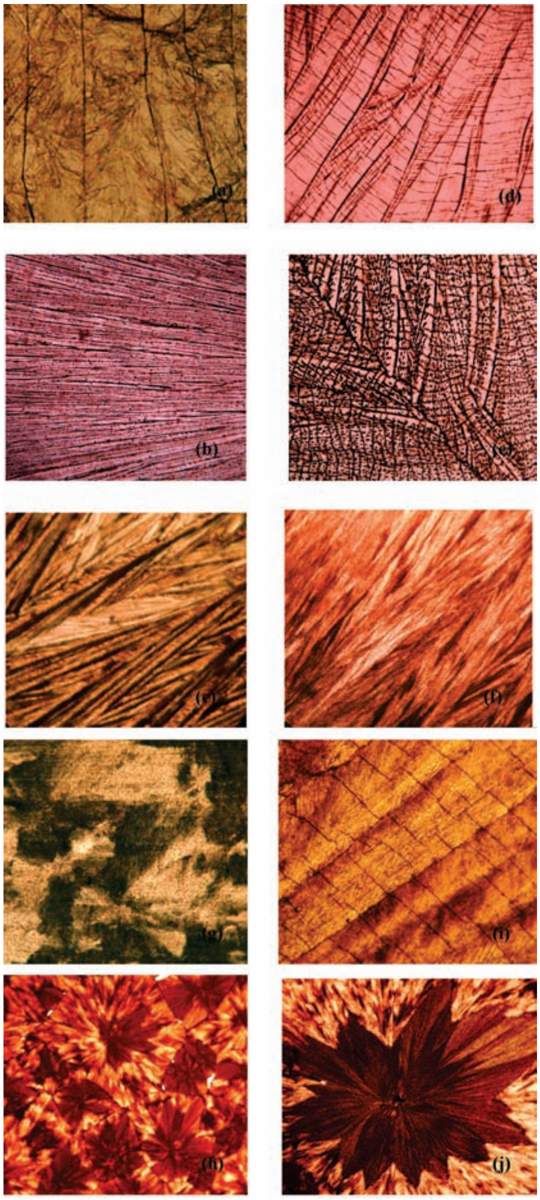

Figure 4. Microstructures for the naphthalen-2-ol + 1,3-dinitrobenzene eutectic system. (a) Naphthalen-2-ol anisotropic, (b) 1,3-dinitrobenzene anisotropic, (c) naphthalen-2-ol + 1,3-dinitrobenzene eutectic anisotropic, (d) naphthalen-2-ol isotropic, (e) 1,3-dinitrobenzene isotropic, (f) naphthalen-2-ol + 1,3-dinitrobenzene eutectic isotropic, (g) naphthalen-2-ol + 1,3-dinitrobenzene hypoeutectic anisotropic, (h) naphthalen-2-ol + 1,3-dinitrobenzene hypereutectic anisotropic, (i) naphthalen-2-ol + 1,3-dinitrobenzene hypoeutectic isotropic, (j) naphthalen-2-ol + 1,3-dinitrobenzene hypereutectic isotropic.

whether the enthalpy of fusion values are additive or not. From Table 4, it is evident that the experimentally determined value of the enthalpy of fusion (14.726 $\text{kJ}\cdot\text{mol}^{-1}$) for the eutectic mixture is lower than the calculated value (21.268 $\text{kJ}\cdot\text{mol}^{-1}$) from the mixture law. The lower enthalpy of fusion value of the eutectic indicates the existence of some interaction between the two components, viz., naphthalen-2-ol and 1,3-dinitrobenzene. Further, it is also evident from Table 4 that the enthalpy of fusion values of naphthalen-2-ol (21.075 $\text{kJ}\cdot\text{mol}^{-1}$) and 1,3-dinitrobenzene (21.203 $\text{kJ}\cdot\text{mol}^{-1}$) are higher than the experimental enthalpy of fusion value of the eutectic mixture. Therefore, the magnitude of interaction between the components in the eutectic mixture is expected to be lower than those present in the individual components. Thus, due to weak interactions, the molecules of naphthalen-2-ol and 1,3-dinitrobenzene may align in a definite way in the eutectic mixture leading to optimized geometry having a sharp melting temperature.

The results obtained for a modulus of rupture indicate that the flexural strengths of the components are very low (Table 2). This may be due to cracking of the sample during isotropic growth. However, the flexural strength of eutectic material [(3.39 ± 0.04) MPa] is much higher in comparison to those of the pure components. Moreover, it is also higher than the flexural strengths of the hypo- and hypereutectics [(1.67 ± 0.01) and (2.059 ± 0.01), respectively]. It seems that the components align in the eutectic mixture in a definite fashion that may give a high flexural strength to the eutectic.

Various physical properties of eutectic materials depend on their crystallization behavior and microstructures. Therefore, an attempt was made to understand the crystallization behavior of naphthalen-2-ol, 1,3-dinitrobenzene, and the eutectic mixture with the help of their microstructures, and the results are given in Figure 4. The anisotropic crystallization pattern of naphthalen-2-ol appears like a wood log when cut horizontally (Figure 4a), whereas 1,3-dinitrobenzene when crystallized anisotropically gives lamellar-type structure with thin lamellae (Figure 4b) and little spacing between the two lamellae. In the case of the eutectic mixture, the anisotropic pattern shows a palm leaf type structure (Figure 4c). The microstructures obtained on isotropic crystallization are completely different from the anisotropic ones. The isotropic microstructures of naphthalen-2-ol, 1,3-dinitrobenzene, and the eutectic mixture show a broken lamellar type structure (Figure 4d), reticulate venation of a *Ficus* leaf type structure (Figure 4e), and a stacked paddy bundle like structure (Figure 4f), respectively. The anisotropic and isotropic microstructures of the naphthalen-2-ol + 1,3-dinitrobenzene eutectic are entirely different from the pure components. The microphotographs of hypo- and hypereutectics were also taken. The anisotropic microstructure of the naphthalen-2-ol + 1,3-dinitrobenzene hypoeutectic appears like a sedimentary rock (Figure 4g), whereas its hypereutectic resembles a cluster of pansy flowers (Figure 4h). On the other hand, on isotropic crystallization, the microstructure of the hypoeutectic appears like the bark of a tree (Figure 4i), and in the case of the hypereutectic, a beautiful floral structure is obtained (Figure 4j). It is not possible to predict the microstructure of the eutectic accurately because the formation of microstructures depends on various factors[13] such as the nature and molecular structure of the components, concentration gradient, interface contact angles, diffusion, nucleation and crystallization characteristics of the two phases, chemical inhomogeneities, and types of defects present in the growing nuclei, and it is difficult to know these parameters precisely; however, Jackson and Hunt[23] were able to predict the structure of the solid/liquid interface of a material in contact with its liquid in terms of roughness parameter (α) of the eutectic system by using eq 5.

$$\alpha = \xi \frac{\Delta_{\text{fus}}H}{RT_{\text{f}}} \tag{5}$$

where ξ is the geometrical coefficient whose value lies between 0.5 and 1.0; $\Delta_{\text{fus}}H$ is the enthalpy of fusion; T_{f} is the temperature; and R is the gas constant. The values of α for the two components and the eutectic mixture were calculated by putting the ξ value equal to 0.5 and 1.0, respectively. The two α values thus obtained are given in Table 4. Both the values of α for the eutectic mixture are greater than 2. Jackson and Hunt[23] have reported that when α > 2 the crystal develops a faceted morphology with an irregular structure.

Conclusion

Phase diagram studies have shown that naphthalen-2-ol and 1,3-dinitrobenzene form a simple eutectic mixture. Linear velocities of crystallization and enthalpies of fusion values have indicated that the eutectic is a nonideal mixture. The flexural strength of the eutectic mixture is found to be higher than that of the components. On the basis of roughness parameters, it is predicted that the eutectic mixture possesses a faceted morphology with an irregular structure.

Literature Cited

(1) Gupta, R. K.; Singh, R. A. Thermochemical and Microstructural Studies on Binary Organic Eutectics and Complexes. *J. Cryst. Growth* **2004**, *26*, 340–347.

(2) Witusiewicz, V. T.; Hecht, U.; Sturz, L.; Rex, S. Phase eqillibria and eutectic growth in ternary organic system amino-methyl-propanediol-(D) camphor-neopentylglycol. *J. Cryst. Growth* **2006**, *286*, 137–145.

(3) Kim, S. G.; Kim, W. T.; Suzuki, T.; Ode, M. Phase-field modeling of eutectic solidification. *J. Cryst. Growth* **2004**, *261*, 135–158.

(4) Suk, M. J.; Leonartz, K. Halo growth during unidirectional solidification of camphor-naphthalene eutectic system. *J. Cryst. Growth* **2000**, *213*, 141–149.

(5) Singh, N. B.; Dwivedi, K. D. Chemistry and Solidification behaviour of Eutectics. *J. Sci. Ind. Res.* **1982**, *41*, 98–116.

(6) Rai, U. S.; Pandey, P. Solidification Behaviour of Binary Organic Eutectics and Monotectics; 1,2,4,5-Tetrachlorobenzene-m-Aminophenol System. *Mater. Lett.* **1999**, *39* (3), 166.

(7) Elliott, R. *Eutectic Solidification Processing*; Butterworth: London, 1983.

(8) Chalmers, B. *Principles of Solidification*; John Wiley and Sons: New York, 1964.

(9) Elder, K. R.; Gunton, J. D.; Martin, G. Nonsothermal Eutectic Crysatillization. *Phys. Rev. E* **1996**, *54* (6), 6476–6484.

(10) Singh, N. B.; Das, S. S.; Singh, N. P.; Agrawal, T. Computer Simulation, Thermodynamic and Microstructural Studies on Benzamide-Benzoic acid Eutectic System. *J. Cryst. Growth* **2008**, *310*, 2878–2884.

(11) Gupta, R. K.; Singh, S. K.; Singh, R. A. Some Physicochemical Studies on Organic Eutectics. *J. Cryst. Growth* **2007**, *300*, 415–420.

(12) Witusiewicz, V. T.; Hecht, U.; Sturz, L.; Rex, S. Phase eqillibria and eutectic growth in ternary organic system (D) camphor-neopentylglycol-succinonitrile. *J. Cryst. Growth* **2006**, *286*, 431–439.

(13) Das, S. S.; Singh, N. P.; Agrawal, T.; Gupta, P.; Tiwari, S. N.; Singh, N. B. Studies of Solidification Behavior and Molecular Interaction in Benzoic Acid-o-Chloro Benzoic Acid Eutectic System. *Mol. Cryst. Liq. Cryst.* **2009**, *501* (1), 107–124.

(14) Singh, N. B.; Agrawal, T.; Gupta, P.; Das, S. S. Solidification Behavior of the Benzamide + *O*-Chlorobenzoic Acid Eutectic System. *J. Chem. Eng. Data* **2009**, *54*, 1529–1536.

(15) Singh, N. B.; Giri, D. P.; Singh, N. P. Solid-Liquid Equillibria for p-Dichlorobenzene + p- Dibromobenzene and p-Dibromobenzene + Resorcinol. *J. Chem. Eng. Data* **1999**, *44*, 605–607.

(16) Dean, J. A., Ed. *Lange's Handbook of Chemistry*; McGraw-Hill Book Company: New York, 1985.

(17) Rastogi, R. P.; Verma, K. T. R. Solid-liquid Equilibrium in Solution of Non-Electrolyte. *J. Chem. Soc.* **1956**, 2097–2101.

(18) Rastogi, R. P.; Bassi, P. S. Mechanism on Eutectic Crystallization. *J. Phys. Chem.* **1964**, *68*, 2398–2406.

(19) Callister, W. D, Jr. *Materials Science and Engineering An Introduction*, 6th ed.; John Wiley & Sons, Inc.: New York, 2005; p 412.

(20) Hillig, H. B.; Turnbull, D. Theory of Crystal Growth in Undercooled Pure Liquid. *J. Chem. Phys.* **1956**, *24*, 914–920.

(21) Sharma, B. L.; Kant, R.; Sharma, R.; Tondon, S. Devitations of Binary Organic Eutectic Melts Systems. *Mater. Chem. Phys.* **2003**, *82*, 216–224.

(22) Winegard, W. C.; Majka, S.; Thall, B. M.; Chalmers, B. Eutectic solidification in Metals. *Can. J. Chem.* **1954**, *29*, 320–327.

(23) Hunt, J. D.; Jackson, K. A. Lamellar and Rod Eutectic Growth Trans. *Metall. Soc. AIME* **1966**, *236*, 1129–1142.

Received for review April 13, 2010. Accepted July 26, 2010.

JE100358E